RSC Advances

PAPER

View Article Online
View Journal | View Issue

Cite this: *RSC Adv.*, 2016, **6**, 67400

Self-powered graphene quantum dot/poly(vinylidene fluoride) composites with remarkably enhanced mechanical-to-electrical conversion

Chong Lu,†[a] Lei Zhang,†[a] Chenwen Xu,[a] Zhenzhong Yin,[a] Shaobing Zhou,[a] Jianxin Wang,[a] Rui Huang,[b] Xiaoqi Zhou,[a] Chaoliang Zhang,[c] Weiqing Yang*[a] and Jun Lu*[a]

Received 27th April 2016
Accepted 26th June 2016

DOI: 10.1039/c6ra10831h

www.rsc.org/advances

We report a facile fabrication approach of a self-powered piezoelectric polymer matrix composite which can efficiently convert mechanical, vibrational and hydraulic energy into electricity without any treatment of electrical poling. The hybrid composite, based on poly(vinylidene fluoride) (PVDF) with a luminescent graphene quantum dot (GQD), finalized its self-polarization process by high pressure crystallization. The size-distributed GQD aggregates *in situ* catalyzed the self-assembly of PVDF molecules into crystalline beta form 1D nanowires and 3D micro/nanowire architectures concurrently at high pressure. Based on these, we have developed some simple piezoelectric generators. The corresponding open-circuit voltage and short-circuit current generally increased with the increase of GQD loadings. Among them, the GQD/PVDF (3/97, wt/wt) composite revealed more than four times larger electrical output if compared to the pure PVDF. Therefore, these unique self-assembled structures evidently enabled a remarkably improved electrical output during the composite deformation. Furthermore, by modulating GQD concentration together with chemical etching, controllable wettability was observed on the surfaces of the pressure-crystallized GQD/PVDF composites, due to the competition effect between enhanced surface roughening and exposed micro/nanoscale polar crystalline hierarchical structures. The study presented here may open a new avenue for the design and mass production of novel self-powered multifunctional polymer matrix composites with self-reinforcement.

Introduction

The self-powered composite structures, able to capture trace amounts of energy from the ambient environment and transform it into electrical energy, have recently attracted considerable attention from the materials research community.[1–6] Among the developed materials and technologies for kinetic energy harvesting, employing piezoelectric generator composites has shown more promise in the conversion of mechanical energy with variable amplitude and frequency into electricity, mainly due to their unique advantages, such as large power density, easy application, and so on.[7,8] Various micro/nanostructured piezoelectric materials, such as ZnO,[2,7,9–11] $BaTiO_3$,[12] alkaline niobate-based particles (KNLN),[13] and $(1-x)Pb(Mg_{1/3}Nb_{2/3})O_3$-$XPbTiO_3$ (PMN-PT),[14] fabricated in a variety of forms, were incorporated in organic or inorganic matrixes for the realization of nanocomposites[2,7,9–14] or macro-fiber composites (MFC)[15] with enhanced piezoelectricity. Particularly, since a flexible polymeric matrix prevents the embedded piezoelectric fillers from breaking and cracking under mechanical stress,[14] there have been attempts to combine piezoelectric macro/nanofillers with polymers, such as polyurethane,[7] SU-8 polymer,[9] polydimethylsiloxane (PDMS),[10,11,14] and PVDF.[12,15] This makes it possible to create novel piezoelectric composites that exhibit the properties of the piezoelectric macro/nanostructures while take advantages of the easy processability of polymers. Nevertheless, major challenges still lie in developing simple, effective and scalable fabrication process and simplifying interface control between inorganic macro/nanostructures and polymer matrixes.[16]

PVDF and its copolymers with trifluoroethylene are one of the limited known piezoelectric class of polymers that promise applicability in stretchable nanogenerators because of their chemical resistance, structural flexibility, processing simplicity,

---

[a] *Key Laboratory of Advanced Technologies of Materials, Ministry of Education, School of Materials Science and Engineering, Southwest Jiaotong University, Chengdu 610031, Sichuan, China. E-mail: junluprc@hotmail.com; wqyang@swjtu.edu.cn; Fax: +86 28 8760 0454; Tel: +86 28 8760 2714*

[b] *College of Polymer Materials Science and Engineering, Sichuan University, Chengdu 610065, Sichuan, China*

[c] *State Key Laboratory of Oral Diseases, West China Hospital of Stomatology, Sichuan University, Chengdu 610041, China*

† These authors equally contributed to this work.

and large piezoelectric coefficients.[16–21] The PVDF-based polymers exhibit a pronounced polymorphism, transforming between several crystal forms under certain conditions, and successful development of piezoelectric polymer devices depends on the effective fabrication of polar crystalline structures, such as β and γ.[20,21] Compared with its copolymer counterpart, *i.e.* poly(vinylidenefluoride-*co*-trifluoroethylene) (P(VDF-TrFE)), in which the β form structure is most thermodynamically favored, commonly piezoelectric activity can not be realized for PVDF homopolymer until it endures an electrical poling process to align the randomly oriented molecular CH_2/CF_2 dipoles along the electrical field direction.[18,19] This results in a non-effective complex fabrication process with undesirable problems, such as substantial additional power consumption, and electrical breakdown failure.[18] Also, electrical poling is not always practical for products with certain desirable shapes or specific applications, though it may be applicable for ultrathin polymeric films.[18,19] Recently, several techniques have been demonstrated in the fabrication of β phase containing PVDF films without electrical poling, including doping with hydrated salt or DNA,[18] and Langmuir–Blodgett deposition.[19]

Graphene quantum dots (GQDs), possessing one or a few layers of graphene with chemical groups connected on the edges, are anisotropic zero dimensional (0D) nanostructured carbon materials with lateral dimensions larger than their height.[23–25] The fluorescent GQDs can be converted through top-down nanocutting methods and bottom-up self-assembly approaches, such as carving graphene or carbon nanotubes (CNTs), and cage-opening and assembling of fullerene C_{60}.[23–25] Size-dependent electron transport was observed for the GQDs with sizes larger than 100 nanometers, smaller than 100 nanometers, and only a few nanometers.[23] Owing to quantum confinement and edge effects, the GQDs have presented extraordinary properties, such as versatile photoluminescence, large surface area, high photostability, low cytotoxicity, and excellent biocompatibility.[26] Hereby GQD-based materials have become the research focus in recent years, and they are being exploited for energy-related devices, composite materials, and environmental and biological applications.[25,26]

For the piezoelectric polymer matrix macro/nano-composites, surface modifying of the macro/nanostructures or use of special macro/nanostructures plays a key role in the enhancement of electrical signal generation.[14] One dimensional (1D) inorganic piezoelectric macro/nanowires and their three dimensional (3D) assemblies have demonstrated their efficiency in direct energy conversion from mechanical motion to electrical power.[1,2,14,15] In this work, GQD/PVDF hybrid composites, with size-distributed aggregates of GQDs formed in the polymer matrix, were fabricated, and polymeric 1D nanowires and 3D micrometer-sized hierarchical structures, both with piezoelectric crystalline β phase, were crystallized simultaneously during the followed up high pressure treatment. Without any treatment of electrical poling, the *in situ* formed piezoelectric polymeric macro/nanostructures enabled a remarkably enhanced mechanical-to-electrical output during the composite deformation. Furthermore, controllable hydrophilic/hydrophobic surfaces were achieved for the pressure-crystallized GQD/PVDF composites by controlling GQD concentration together with chemical etching.

Experimental part

GQD powder with photoluminescence was supplied by Shanghai Simbatt Energy Technology Co., Ltd, and used as received. The GQDs, with 80–90 at% C and 10–20 at% O/N, possess 1–5 layers of graphene, 1–2 nm thickness and 5–15 nm lateral dimensions. PVDF powder, commercial-grade Solef 6010, was supplied by Solvay Co., Ltd, Belgium. The corresponding weight-average molecular weight, M_w, was 322 000 g mol^{-1}. An analytical grade *N*,*N*-dimethylformamide (DMF) was provided by Chengdu Kelong Chemical Co., Ltd. PVDF solution was prepared by dissolving PVDF powder in DMF with stirring at 60 °C, and then GQD powder was added into the PVDF/DMF solution, followed by 2 h mechanical stirring and 4 h ultrasonication at room temperature. The GQD/PVDF/DMF suspensions, with different GQD concentrations, were respectively coated on glass substrates, and subsequently dried in a vacuum oven at 70 °C for 3 h to remove the DMF solvent.

High-pressure experiments for the GQD/PVDF composites, fabricated by solution casting approach, were carried out with a self-made piston-cylinder apparatus.[27] The following procedure for crystallization was used. After loading the samples, the temperature was increased to 200 °C to allow them to be melted. Then a low pressure (150 MPa) was applied, and the temperature was raised to 230 °C. After equilibrium was established, the pressure was further raised to 300 MPa. These samples were kept under these conditions for 30 min, and then quenched down to ambient condition. The GQD/PVDF specimens, with column aspect, 8.04 mm in diameter and 0.66 mm in thickness, were prepared by varying GQD loadings (Fig. 1). For reference, a pure PVDF sample was also prepared under the same high pressure treatment.

Transmission electron microscopy (TEM) detections were performed with a JEOL JEM-2100F apparatus. Differential scanning calorimetry (DSC) measurements were conducted at atmospheric pressure by using a TA-Q20 instrument. Wide-angle X-ray diffraction (WAXD) results were obtained at room temperature with a DX-1000 diffractometer. Attenuated total reflectance Fourier transform infrared spectroscopy (ATR-FTIR) data were obtained using a Nicolet 5700 spectrometer. After the WAXD and ATR-FTIR characterizations, the sample surfaces were etched by using a method modified from that developed by Vaughan,[28] and then coated with gold for scanning electron microscopy (SEM) observations using a JSM-6330F apparatus. The contact angles (CAs) of water droplets that had been placed onto the sample surfaces were measured using a KRUSS DSA100 optical contact angle measuring device.

The energy harvesting performance of the samples, without any electrical poling applied, was evaluated by periodic impacting test, as shown in Fig. 1, which presents a schematic diagram of the measurement system. With a NTI AG HS01-37 × 166 linear motor as the impact source, the generated electrical outputs, *i.e.* open-circuit voltage and short-circuit current, were collected using a Keithley 6514 system electrometer and a Stanford Research SR570 low-noise current preamplifier, respectively.

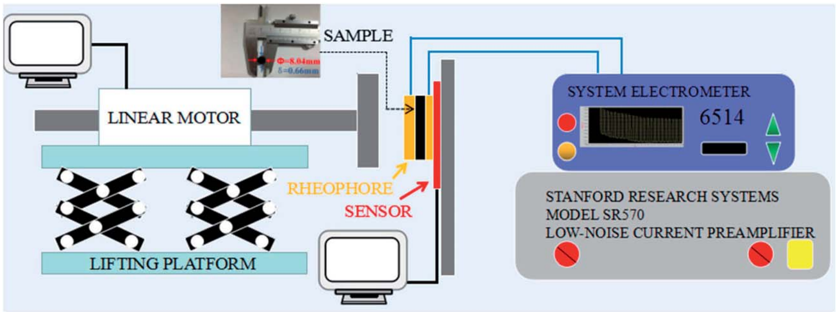

Fig. 1 Schematic diagram of the impact measurement system for concurrently collecting the electrical potential and current output, generated during the dynamic load of the GQD/PVDF composites.

Results and discussion

Fig. 2a shows the optical images of a DMF solution containing GQDs, under UV- and visible-light irradiation, respectively. The GQD solution fluoresced with an excitation wavelength of 365 nm from a UV lamp. Fig. 2b gives out the typical TEM photograph of the as-fabricated GQD/PVDF with 3 wt% loading of the fluorescent GQDs, prior to the treatment by high pressure. As can be seen, the GQDs generally achieved a distribution within nanoscale in the polymer matrix. Nevertheless, the GQDs intrinsically tend to aggregate, and GQD agglomerations, with size distributed from a few nanometers to several tens of nanometers, were formed during the composite fabrication. Although the size and amount of the aggregates decrease with the decrease of GQD loadings, there are still agglomerates, in a size distribution fashion, observed for the GQD/PVDF composites (Fig. 2c and d).

Fig. 3a represents the DSC results of the GQD/PVDF composite samples with different GQD concentration, crystallized at 300 MPa and 230 °C for 30 min. Two melting peaks, with a shoulder formed on the high-temperature side of the high temperature endotherm, were observed on the curve of the GQD/PVDF (1/99, wt/wt) sample. Both the low and high temperature peaks shifted to higher temperatures when the GQD loading reached 2 wt%. Moreover, the high melting point (186.38 °C) for the GQD/PVDF (2/98, wt/wt) was 12 °C higher than that of the referenced pure PVDF (174.06 °C). Nevertheless, with the GQD loading further increased to 3 wt%, only single endotherms emerged on the DSC profile. This indicated that crystal form transforming together with morphological variation occurred with the GQD loading increase.[27,29]

Commonly, the identification of the crystalline phases of PVDF is carried out by WAXD and/or FTIR measurements. The corresponding WAXD and ATR-FTIR data of the GQD/PVDF composite samples are shown in Fig. 3b and c, respectively. Referring to the X-ray diffraction data,[27,29] the apparent single peak of orthorhombic β phase, at 2θ angle 20.4–21.1°, actually coming from the superposition of the (110) and (200) reflections, was observed on the profiles of these pressure crystallized GQD/PVDF samples. Moreover, for IR bands, those at 840 and 1280 cm^{-1}, characteristic of the β phase, further confirmed that β phase should be induced in the composites.[27,29] We also noted the coexistence of β phase with other crystalline forms of the polymer, *i.e.* α and γ phase, as suggested by the corresponding characteristic reflections in WAXD and IR spectra.

The results in Fig. 3a suggested the crystallization behavior for the composite with 1 wt% GQD loading was drastically different from other three samples. This was mainly attributed to a relative large scale formation of γ phase crystals. As confirmed by the IR spectra (Fig. 3c), the intensity for the band characteristic of γ phase at 1234 cm^{-1} is the strongest for the tested GQD/PVDF (1/99, wt/wt) sample. To investigate the pressure effect on the phase transition of the GQD/PVDF (1/99, wt/wt) composite, three samples, respectively, were also prepared at 200, 400 and 500 MPa, with other conditions being the same, and the characterization results are shown in Fig. 4. The melting point of the polymer was not further increased by varying pressure (Fig. 4a). Also, the content of γ phase crystals increased with the increase of pressure during 200–400 MPa, and then decreased when the pressure was further increased to 500 MPa (Fig. 4b and c). Although α phase was not completely

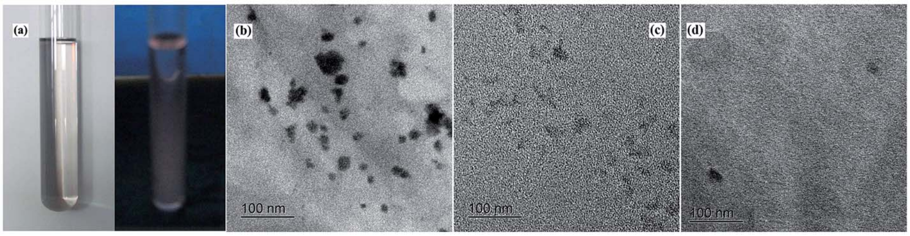

Fig. 2 Photographs for a DMF solution of the GQDs under sunlight (a, left) and at 365 nm UV excitation (a, right), and the representative TEM images for the as fabricated GQD/PVDF composites with 3.0 wt% (b), 2.0 wt% (c) and 1.0 wt% (d) GQD loadings, respectively.

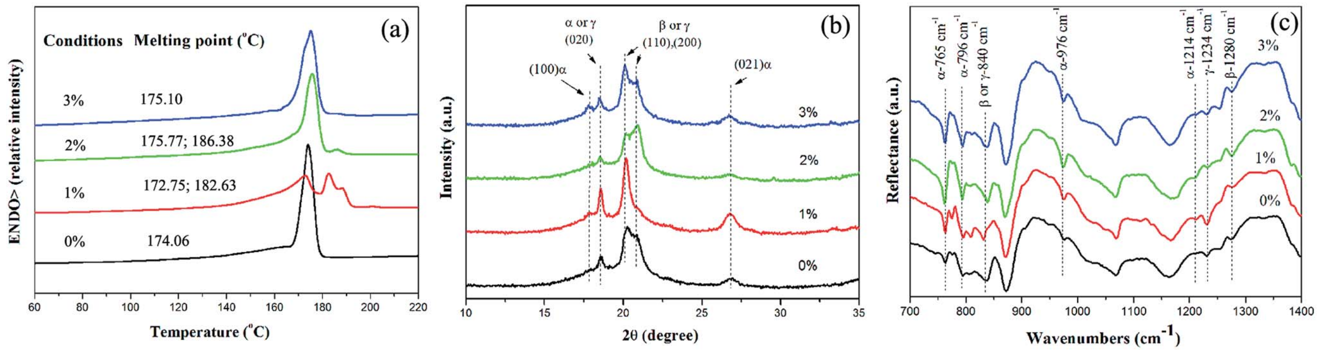

Fig. 3 DSC (a), WAXD (b) and ATR-FTIR (c) results of the GQD/PVDF composite samples, with different GQD concentration, crystallized at 300 MPa, 230 °C for 30 min.

removed from the sample, the intensity of the IR peak at 1280 cm^{-1}, representative of crystalline β phase, increased with the increase of pressure (Fig. 4c).

Although the above DSC, WAXD and IR data (Fig. 3) indicated that morphological variable β phase structures were obtained in the GQD/PVDF samples by varying GQD loadings, direct morphologies should be given with SEM measurements. Recently, C_{60} and CNT agglomerations were utilized by us to induce the self-assembly of PVDF molecules, and 1D nanowires and their 3D micro/nanoscale architectures of the polymer, both with piezoelectric crystalline β phase, were formed in the high pressure crystallized C_{60}/PVDF and CNT/PVDF composites, respectively.[27,29] Fig. 5a shows the SEM image of the etched surface of the GQD/PVDF (1/99, wt/wt) sample, in which the fern-branch 3D hierarchical polymeric structures, with individual featured β phase macro/nanowires extending in various directions, were clearly revealed. More such micro/nanowire assemblies were crystallized by increasing the GQD loadings in GQD/PVDF composites (Fig. 5b). Particularly, as designated in Fig. 5c, the micro/nanoscale assemblies began to connect when the GQD loading was increased to 3 wt%. This finally *in situ* promoted the formation of a hierarchically structured network in the composite, totally composed of the 3D micro/nanowire assemblies with crystalline β phase. Furthermore, in addition to the 3D architectures, the piezoelectric β form crystalline 1D nanowires of the polymer were simultaneously crystallized in the GQD/PVDF composites. Fig. 6 represents the typical morphology of such nanowires with a rectangular cross-section, obviously revealing their uniform size and morphology achieved after high pressure crystallization.

Although the WAXD and IR spectra in Fig. 3b and c suggested that crystalline β phase was also crystallized in the pure PVDF, the nanowires and micro/nanowire clusters of the polymer were firstly observed in the GQD/PVDF composites only after the high pressure treatment. A comparison experiment was also conducted for the original neat PVDF, prior to the applied high pressure crystallization, and the GQD/PVDF composites, fabricated just by the solution casting approach, and the representative results were shown in Fig. 7. The DSC and WAXD suggested that the melting enthalpy of PVDF was increased by the incorporation of GQDs (Fig. 7a and b). However, the melting points were almost the same (Fig. 7a). Furthermore, no crystalline β phase crystal, which is essential in the creation of piezoelectricity of the polymer, was crystallized during the solution casting of the GQD/PVDF composites (Fig. 7b and c). Therefore, the concurrent growth of both the 1D nanowires and 3D micro/nanowire architectures should be mainly attributed to a size-distributed GQD-induced self-assembly of PVDF molecular chains at high pressure. Similar to the role of Sn balls in the growth of ZnO nanostructures,[30] the GQDs plays as a catalyst *in situ*. The tiny GQD aggregates catalyzed the assembly of PVDF into nanowires, while the GQD

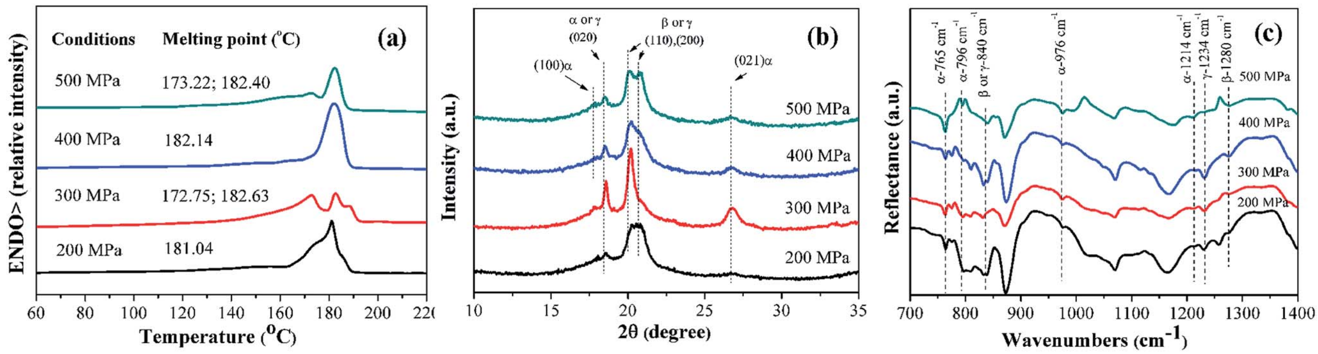

Fig. 4 DSC (a), WAXD (b) and ATR-FTIR (c) results of the GQD/PVDF (1/99, wt/wt) composite samples, crystallized at different pressure, 230 °C for 30 min.

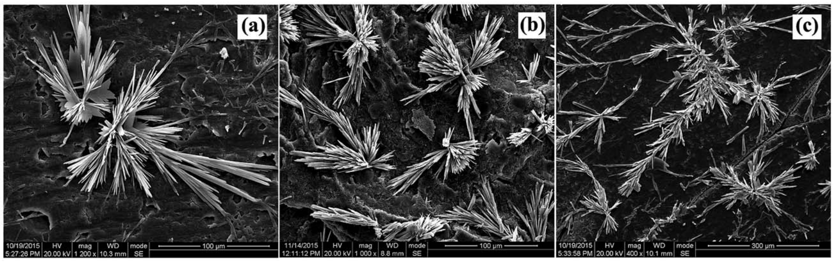

Fig. 5 SEM images of the etched fracture surfaces of GQD/PVDF composite samples, with 1.0 wt% (a), 2.0 wt% (b) and 3.0 wt% (c) GQD loadings, respectively, crystallized at 300 MPa, 230 °C for 30 min.

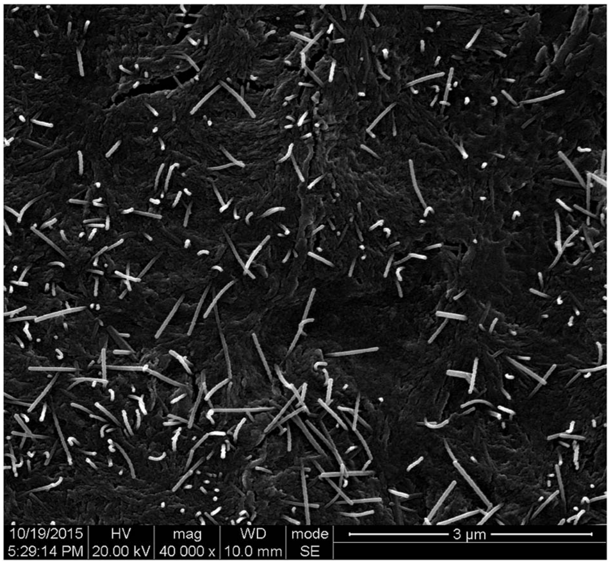

Fig. 6 SEM image of the etched fracture surface of a GQD/PVDF (2/98, wt/wt) composite sample, crystallized at 300 MPa, 230 °C for 30 min.

agglomerations with larger size can simultaneously induce the formation of numerous nanowires and then result in the radial fuzzy hierarchical micro/nanowire assemblies.

It is known that unusual structural features at the micro/nanometer scale may enable material surfaces in controlling their interaction with liquids and hence wettability.[22,31] Fig. 8 shows the wettability results on the surfaces of the pressure crystallized GQD/PVDF composite samples, before and after etching, by utilizing distilled water as the test liquid. The surface of the referenced original pure PVDF repelled the water droplet, and showed high hydrophobicity. The introduction of GQDs enhanced the surface roughness, and the surface hydrophilicity of the GQD/PVDF, without chemical etching applied, increased with the increase of GQD loadings. The hydrophilic properties, for both PVDF and GQD/PVDF composites, were improved by the delicate etching process, and the CAs decreased substantially. The hydrophobic-to-hydrophilic conversion was observed for the referenced PVDF, and its etched surface was high hydrophilicity. This was ascribed to the exposure of the crystalline phases in the sample, which further sharply enhanced its surface roughness. It is intriguing that the CAs of the etched GQD/PVDF surfaces increased with the increase of GQD loadings. The increasing CAs should be assigned to the exposure of more and more flower-like micro/nanoscale polar crystalline hierarchical structures (Fig. 5). The intricate micrometer-sized micro/nanostructured patterns were reported to be a class of textures with superhydrophobic self-cleaning lotus effect.[22,31] However, we noted that their CA values were still respectively smaller than those of the original surfaces by a relative large margin, due to the competition effect between enhanced surface roughening and exposed micro/nanoscale hierarchical structures.

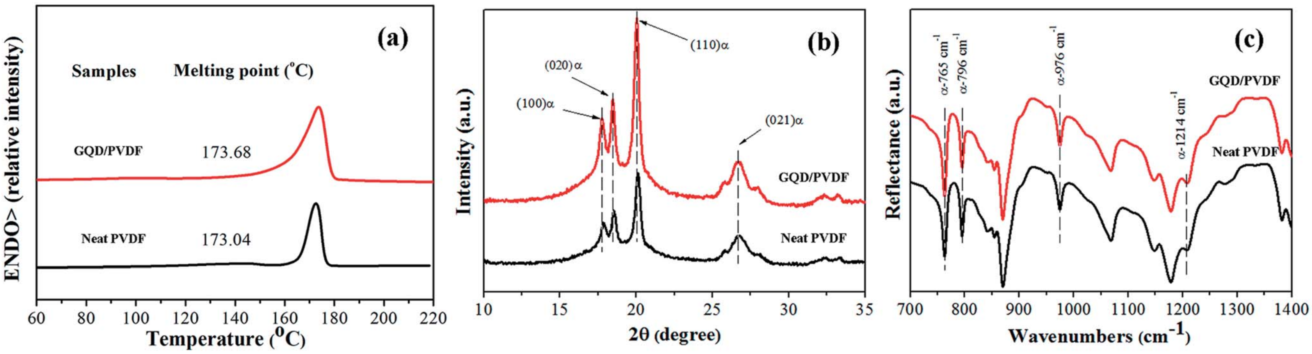

Fig. 7 DSC (a), WAXD (b) and ATR-FTIR (c) results of the GQD/PVDF (0.5/99.5, wt/wt) composite sample, fabricated by the solution casting approach, and the original neat PVDF, respectively.

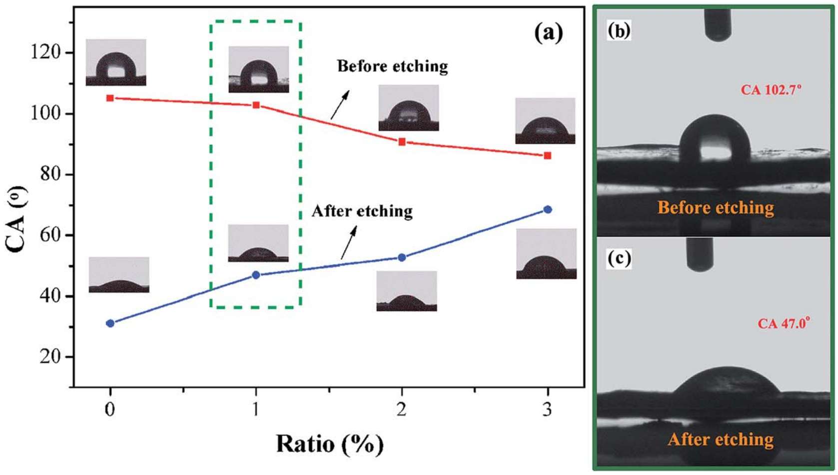

Fig. 8 Wettability results on the surfaces of the GQD/PVDF composite samples, with different GQD concentration, crystallized at 300 MPa, 230 °C for 30 min. As signalized by a green frame in (a), (b) and (c) are snapshots captured by a video contact angle measuring instrument during the test of a GQD/PVDF (1/99, wt/wt) composite sample, before and after etching, respectively.

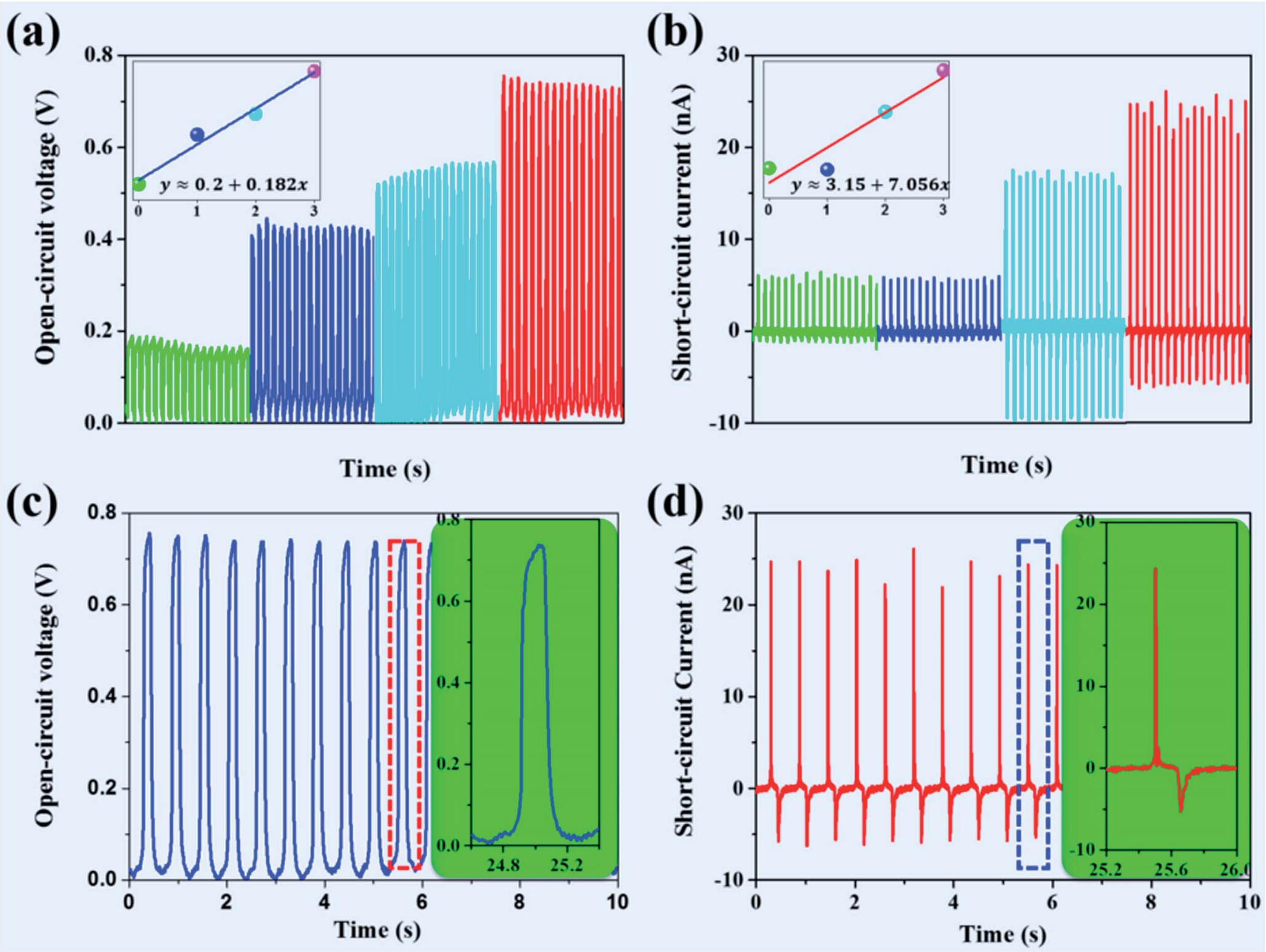

Fig. 9 Electrical measurement results for the high pressure crystallized GQD/PVDF composites. (a) Open-circuit voltage and (b) corresponding short-circuit current, respectively, generated by various GQD/PVDF composites under a 1.7 Hz 150 N impact. The insets in (a) and (b) show the dependence of the voltage and current on GQD loading, respectively. The points represent peak values of electrical signals, and the lines are fitted results. (c) Open-circuit voltage and (d) short-circuit current, respectively, generated by a GQD/PVDF (3/97, wt/wt) composite sample. The insets are enlarged views for one cycle.

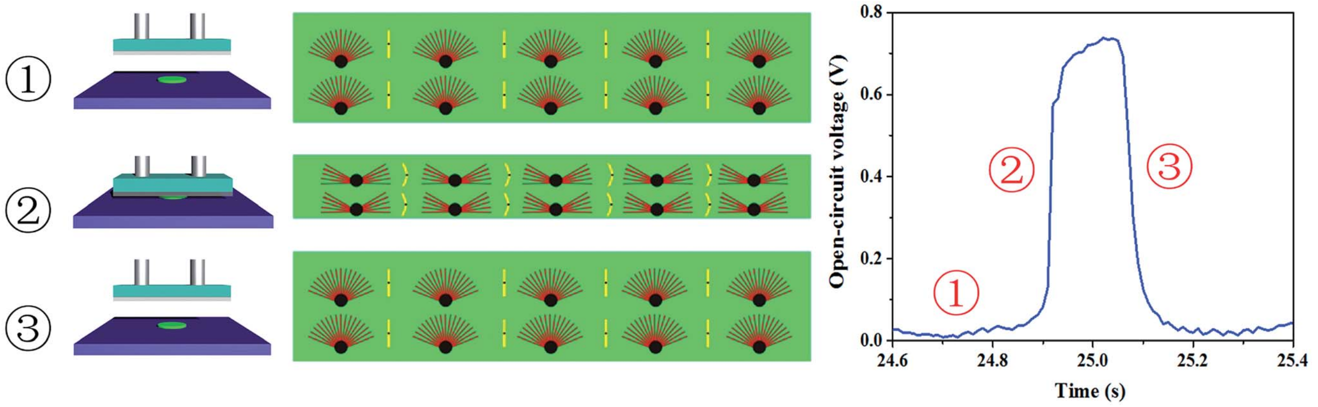

Fig. 10 Schematic representation of the procedure for generating electricity by deforming the *in situ* formed piezoelectric 3D micro/nanowire assemblies and 1D nanowires simultaneously with low frequency impact.

The electrical potential and current output of the high pressure crystallized GQD/PVDF composite samples, without any treatment of electrical poling, were measured under low frequency impact, with a standard vibration system as the vibration source, which is a simple evaluating method representative of the actual application of energy-harvesting piezoelectric generators. Fig. 9a and b show the open-circuit voltage and short-circuit current of the piezoelectric generators based on various GQD/PVDF composites under the same conditions of 1.7 Hz and 150 N impacts. The insets suggested that both the voltage and current increased almost linearly with the increase of GQD loadings, evidently demonstrating the excellent tuning ability of GQDs for the electric output of GQD/PVDF composites. Particularly, open-circuit voltage and short-circuit current of a GQD/PVDF sample with 3 wt% GQD loading were, respectively, up to 0.75 V and 25.7 nA, which were more than four times larger than those of the pure PVDF. According to the calculation, an as-fabricated GQD/PVDF (3/97, wt/wt) sample with just only 0.067 cm^3 volume equals a 1.5 V battery commonly used in our daily life. Fig. 9c and d present the snapshots of the voltage and current curves for the GQD/PVDF (3/97, wt/wt) sample. The composite sample responded harmonically to the low frequency impact excitation. For the open-circuit voltage, the direct impact of the stress caused the rising of the voltage to a peak value, and a large positive peak was generated. Also, the subsequent relaxation of the stress, occurring when the initial stress was removed, resulted in the falling of the voltage and then the formation of an almost negligible negative peak. As for the consistent short-circuit current, it revealed more characteristics of alternating current (AC). Positive and negative pulses were generated, respectively, by the direct impact and the relaxed stress from the damping effect. Apart from the role as a generator, it was reported that the piezoelectric micro/nanocomposites can also serve as a capacitor.[14] This resulted in the much larger difference for the positive and negative voltage peaks, if compared with that between the corresponding current peaks.

The remarkably enhanced power output during the electromechanical conversion of the GQD/PVDF composites, especially for the sample with a high GQD loading level, may be attributed to the *in situ* growth of the unique piezoelectric hierarchical micro/nanostructures. The composites finalized their self-polarization process through the formation of micro/nanostructures with crystalline β phase, induced by the size distributed GQDs at high pressure. To summarize the key role of the micro/nanostructures in the electricity generation during the composite deformation under a dynamic loading, a schematic illustration is presented in Fig. 10. The *in situ* crystallized micro/nanostructures, including the 1D nanowires and their 3D micro/nanoscale assemblies, deform together with the polymeric matrix when the composite sample is compressed. The macro/nanostructures with special morphologies enhance the efficiency of mechanical-to-electrical conversion, with the matrix transferring stress to its active inclusions. Charges are generated, and flow through the electrodes and then build up an output voltage between the positive and negative contacts. When the initial stress is removed, the recovery of the matrix to the original position enables the micro/nanostructures changing from a compressed state to a relaxed state. This results in a negative output voltage, due to the moving back of the charges in the opposite direction.

Conclusion

In summary, a novel self-powered hybrid composite, based on GQDs and PVDF, has been fabricated by a facile approach. The GQD/PVDF composites finalized their self-polarization at high pressure, through a size-distributed GQD-induced growth of a hierarchically structured network, totally composed of the 1D nanowires and 3D micro/nanowire assemblies with crystalline β phase. The *in situ* formed macro/nanostructures with special morphologies remarkably enhanced the efficiency of mechanical-to-electrical conversion. Compared to the pure PVDF, more than four times larger electrical output was revealed for a GQD/PVDF composite, without any treatment of electrical poling. Moreover, the pressure crystallized unusual structural features at the micro/nanometer scale enabled the achieving of controllable hydrophilic/hydrophobic surfaces for the GQD/PVDF composites. We believe the present study may make a considerable contribution to the development of the mass processing technologies for self-powered piezoelectric polymer matrix composites, especially for those with desirable complex shapes for special applications.

Author contributions

Jun Lu conceived the idea, and initiated the study. Chong Lu, Lei Zhang, Chenwen Xu, Zhenzhong Yin, Shaobing Zhou, Jianxin Wang, Rui Huang, Xiaoqi Zhou and Chaoliang Zhang carried out the sample preparation and characterization. Jun Lu and Weiqing Yang organized the entire research, analysed and interpreted the data, and wrote the manuscript with the assistance of all other co-authors. All authors discussed the results and commented on the manuscript.

Conflict of interest

The authors declare no competing financial interest.

Acknowledgements

This work was supported by the National Natural Science Foundation of China (No. 51373139) and technological projects for Distinguished Young Scholars of Sichuan Province (No. 2015JQ0013). The authors extended their gratitude to Professor Wei Yang and Dr Yajiang Huang (Sichuan University) for valuable discussions.

References

1 Z. L. Wang and J. Song, Piezoelectric nanogenerators based on zinc oxide nanowire arrays, *Science*, 2006, **163**, 242–246.

2 Y. Qin, X. D. Wang and Z. L. Wang, Microfibre-nanowire hybrid structure for energy scavenging, *Nature*, 2008, **451**, 809–813.

3 Z. L. Wang, Triboelectric nanogenerators as new energy technology for self-powered systems and as active mechanical and chemical sensors, *ACS Nano*, 2013, **7**, 9533–9537.

4 F. Zhang, Y. Zang, D. Huang, C. A. Di and D. Zhu, Flexible and self-powered temperature-pressure dual-parameter sensors using microstructure-frame-supported organic thermoelectric materials, *Nat. Commun.*, 2015, **6**, 8356.

5 S. Yoshino, T. Miyake, T. Yamada, K. Hata and M. Nishizawa, Molecularly ordered bioelectrocatalytic composite inside a film of aligned carbon nanotubes, *Adv. Energy Mater.*, 2013, **3**, 60–64.

6 H. W. Yu, H. K. Kim, T. Kim, K. M. Bae, S. M. Seo, J. M. Kim, T. J. Kang and Y. H. Kim, Self-powered humidity sensor based on graphene oxide composite film intercalated by poly(sodium 4-styrenesulfonate), *ACS Appl. Mater. Interfaces*, 2014, **6**, 8320–8326.

7 H. Souri, I. W. Nam and H. K. Lee, A Zinc oxide/polyurethane-based generator composite as a self-powered sensor for traffic flow monitoring, *Compos. Struct.*, 2015, **134**, 579–586.

8 D. Pan, F. Dai and H. Li, Piezoelectric energy harvester based on bi-stable hybrid symmetric laminate, *Compos. Sci. Technol.*, 2015, **119**, 34–45.

9 M. Kandpal, C. Sharan, P. Poddar, K. Prashanthi, P. R. Apte and V. R. Rao, Photopatternable nano-composite (SU-8/ZnO) thin films for piezo-electric applications, *Appl. Phys. Lett.*, 2012, **101**, 104102.

10 B. Saravanakumar, K. Thiyagarajan, N. R. Alluri, S. S. Yoon, K. Taehyun, Z. H. Lin and S. J. Kim, Fabrication of an eco-friendly composite nanogenerator for self-powered photosensor applications, *Carbon*, 2015, **84**, 56–65.

11 J. Chun, N. R. Kang, J. Y. Kim, M. S. Noh, C. Y. Kang, D. Choi, S. W. Kim, Z. L. Wang and J. M. Baik, Highly anisotropic power generation in piezoelectric hemispheres composed stretchable composite film for self-powered motion sensor, *Nano Energy*, 2015, **11**, 1–10.

12 J. Nunes-Pereira, V. Sencadas, V. Correia, J. G. Rocha and S. Lanceros-Méndez, Energy harvesting performance of piezoelectric electrospun polymer fibers and polymer/ceramic composites, *Sens. Actuators, A*, 2013, **196**, 55–62.

13 C. K. Jeong, K. I. Park, J. Ryu, G. T. Hwang and K. J. Lee, Large-area and flexible lead-free nanocomposite generator using alkaline niobate particles and metal nanorod filler, *Adv. Funct. Mater.*, 2014, **24**, 2620–2629.

14 S. Xu, Y. W. Yeh, G. Poirier, M. C. McAlpine, R. A. Register and N. Yao, Flexible piezoelectric PMN-PT nanowire-based nanocomposite and device, *Nano Lett.*, 2013, **13**, 2393–2398.

15 Y. Yang, L. Tang and H. Li, Vibration energy harvesting using macro-fiber composites, *Smart Mater. Struct.*, 2009, **18**, 115025.

16 J. H. Lee, H. J. Yoon, T. Y. Kim, M. K. Gupta, J. H. Lee, W. Seung, H. Ryu and S. W. Kim, Micropatterned P(VDF-TrFE) film-based piezoelectric nanogenerators for highly sensitive self-powered pressure sensors, *Adv. Funct. Mater.*, 2015, **25**, 3203–3209.

17 Z. Pi, J. Zhang, C. Wen, Z. B. Zhang and D. Wu, Flexible piezoelectric nanogenerator made of poly(vinylidenefluoride-*co*-trifluoroethylene) (PVDF-TrFE) thin film, *Nano Energy*, 2014, **7**, 33–41.

18 A. Tamang, S. K. Ghosh, S. Garain, M. M. Alam, J. Haeberle, K. Henkel, D. Schmeisser and D. Mandal, DNA-assisted β-phase nucleation and alignment of molecular dipoles in PVDF film: a realization of self-poled bioinspired flexible polymer nanogenerator for potable electronic devices, *ACS Appl. Mater. Interfaces*, 2015, **7**, 16143–16147.

19 S. Chen, X. Li, K. Yao, F. E. H. Tay, A. Kumar and K. Zeng, Self-polarized ferroelectric PVDF homopolymer ultra-thin films derived from Langmuir–Blodgett deposition, *Polymer*, 2012, **53**, 1404–1408.

20 J. Wang, J. Wu, W. Xu, Q. Zhang and Q. Fu, Preparation of poly(vinylidene fluoride) films with excellent electric property, improved dielectric property and dominant polar crystalline forms by adding a quaternary phosphorous salt functionalized graphene, *Compos. Sci. Technol.*, 2014, **91**, 1–7.

21 M. C. García-Gutiérrez, A. Linares, J. J. Hernández, D. R. Rueda, T. A. Ezquerra, P. Poza and R. J. Davies, Confinement-induced one-dimensional ferroelectric polymer arrays, *Nano Lett.*, 2010, **10**, 1472–1476.

22 J. Chen, X. Zhong, J. Lin, I. Wyman, G. Zhang, H. Yang, J. Wang, J. Wu and X. Wu, The facile preparation of self-cleaning fabrics, *Compos. Sci. Technol.*, 2016, **122**, 1–9.

23 L. A. Ponomarenko, F. Schedin, M. I. Katsnelson, R. Yang, E. W. Hill, K. S. Novoselov and A. K. Geim, Chaotic Dirac billiard in graphene quantum dots, *Science*, 2008, **320**, 356–358.

24 J. Lu, P. S. E. Yeo, C. K. Gan, P. Wu and K. P. Loh, Transforming C_{60} molecules into graphene quantum dots, *Nat. Nanotechnol.*, 2011, **6**, 247–252.

25 S. Zhu, Y. Song, X. Zhao, J. Shao, J. Zhang and B. Yang, The photoluminescence mechanism in carbon dots (graphene quantum dots, carbon nanodots, and polymer dots): current state and future perspective, *Nano Res.*, 2015, **8**, 355–381.

26 Z. P. Zhang, J. Zhang, N. Chen and L. T. Qu, Graphene quantum dots: an emerging material for energy-related applications and beyond, *Energy Environ. Sci.*, 2012, **5**, 8869–8890.

27 D. P. Zhang, P. F. Tian, X. Chen, J. Lu, Z. W. Zhou, X. M. Fan and R. Huang, Fullerene C_{60}-induced growth of hollow piezoelectric nanowire arrays of poly(vinylidene fluoride) at high pressure, *Compos. Sci. Technol.*, 2013, **77**, 29–36.

28 A. S. Vaughan, Etching and morphology of poly(vinylidene fluoride), *J. Mater. Sci.*, 1993, **28**, 1805–1813.

29 W. J. Huang, Z. P. Li, P. F. Tian, X. Chen, J. Lu, Z. W. Zhou, R. Huang, T. X. Liu, C. L. Zhang and X. L. Wang, Agglomerated carbon nanotube-induced growth of piezoelectric 3D nanoarchitectures assembled from hollow 1D nanowires of poly(vinylidene fluoride) at high pressure, *Compos. Sci. Technol.*, 2014, **90**, 110–116.

30 R. S. Yang and Z. L. Wang, Growth of self-assembled ZnO nanowire arrays, *Philos. Mag.*, 2007, **87**, 2097–2104.

31 Y. M. Zheng, H. Bai, Z. B. Huang, X. L. Tian, F. Q. Nie, Y. Zhao, J. Zhai and L. Jiang, Directional water collection on wetted spider silk, *Nature*, 2010, **463**, 640–643.